Combustion Synthesis: an Effective Tool for the Synthesis of Advanced Materials

by Umberto Anselmi-Tamburini, Filippo Maglia, Giorgio Spinolo, Z.A. Munir

Combustion synthesis (or SHS) received a considerable attention in the last twenty years as an innovative method for the synthesis of advanced ceramic materials. The paper reviews the main characteristics of this technique. In the first two sections the main parameters controlling the feasibility of the synthesis through combustion are discussed together with some theoretical and modellistic considerations. In the last section a recent development of the technique, allowing its extension towards less exothermic reaction, is discussed in some details.

Combustion synthesis (CS) or Self-propagating High-temperature Synthesis (SHS) have attracted considerable interest in the last two decades due to its unique combination of technologically relevant characteristics [1-8]. The method, in fact, makes possible the rapid synthesis of several highly refractory inorganic materials, thus avoiding the prolonged high temperature treatment usually required in their conventional preparation. In this new approach the synthesis is obtained through an extremely rapid self-sustaining process driven by the large heat release by the synthesis reaction. The macroscopic characteristics of CS processes resemble those observed in conventional combustion processes. The schematic of a typical combustion synthesis process is shown in Figure 1. The reactants, in form of fine powders, are usually dry-mixed and cold-pressed in order to obtain cylindrical pellets. These pellets are then placed in a controlled atmosphere (usually an inert gas) and ignited through an electrically heated coil, a laser beam, or an electric discharge. If the combination of thermochemical and thermophysical properties of the system are appropriate, a high temperature reaction front (1500<T<3500 °C) is initiated which then propagates through the reactants with a rate ranging from some millimeters to several centimeters per second. A variant of this scheme involves one gaseous reactant. In this case the pellet is made of the powders of the other reactant. This approach allows the synthesis of nitrides, hydrides, and oxides. Beside low energy requirements and the high reaction rate, the method has other advantages over the traditional methods, such as the simplicity of the experimental apparatus, particularly the lack of a need for a reaction container. Another demonstrated advantage is represented by the high purity of the products, which is largely due to the expulsion of volatile impurities under the extremely high temperatures in the wave. The reaction products are generally porous, but densification can easily be obtained through the application of a mechanical load just after the end of the reaction or simultaneous to it.

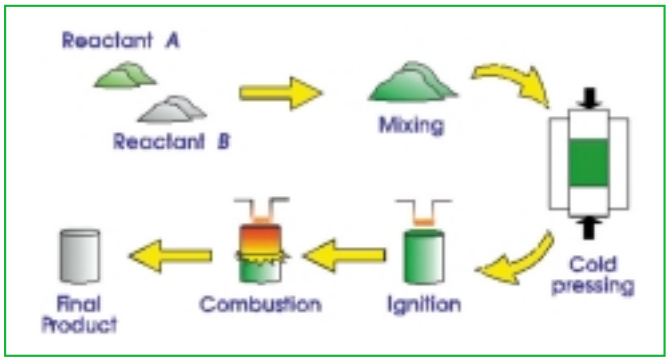

Figure 1 - Schematic of a typical CS process involving only solid reactants

Combustion synthesis has been used to synthesize a large number of monolithic and composite inorganic materials (Table 1). Some of these materials in this table have been used or proposed for use in the following applications [2, 7]:

- abrasives, cutting tools, polishing powders (*e.g.* TiC, cemented carbides, and carbonitrides);
- elements for resistance heating furnaces (*e.g.* $MoSi_2$);
- high temperature lubricants (*e.g.* chalcogenides of Mo);
- neutron attenuators (*e.g.* refractory metal hydrides);
- shape-memory alloys (*e.g.*TiNi);

U. Anselmi-Tamburini, F. Maglia, G.Spinolo, Dipartimento di Chimica fisica e C.S.T.E./CNR - Università di Pavia - V.le Taramelli, 16 - 27100 Pavia; Z.A. Munir, Department of Chemical Engineering and Materials Science - University of California – Davis - CA 95616-5294 - Usa.

Table 1 - [2]

Borides	CrB, HfB_2, NbB_2, TaB_2, TiB_2, LaB_6, MoB_2, WB, ZrB_2, VB, VB_2
Carbides	TiC, ZrC, HfC, NbC, SiC, Cr_3C_2, SiC, B_4C, WC, TaC, VC, Mo_2C
Carbonitrides	TiC-TiN, NbC-NbN, TaC-TaN
Cemented carbides	TiC-Ni, TiC-Mo, WC-Co, Cr_3C_2-(Ni,Mo)
Chalcogenides	MoS_2, $TaSe_2$, NbS_2, WSe_2, $MoSe_2$, MgS
Composites	TiC-TiB_2, TiB_2-Al_2O_3, B_4C-Al_2O_3, TiN-Al_2O_3, TiC-Al_2O_3, $MoSi_2$-Al_2O_3, Ni-ZrO_2
Hydrides	TiH_2, ZrH_2, NbH_2
Intermetallics	NiAl, $NiAl_3$, FeAl, NbGe, TiNi, CoTi, CuAl
Nitrides	TiN, ZrN, BN, AlN, Si_3N_4, TaN (cubic and exagonal)
Silicides	$MoSi_2$, $TaSi_2$, Ti_5Si_3, $ZrSi_2$, WSi_2, $NbSi_2$
Oxides	ZrO_2, YSZ, $MgAl_2O_4$, $Bi_4V_4O_{11}$, $YBa_2Cu_3O_{7-x}$

- high temperature structural alloys (*e.g.* Ni-Al intermetallic compounds);
- steel melting additive (*e.g.* nitrided ferroalloys);
- electrodes for electrolysis of corrosive media (*e.g.* TiN);
- coating for containment of liquid metals and corrosive metals (*e.g.* products of aluminum and iron oxide thermite reactions);
- powders for further ceramic processing (*e.g.* Si_3N_4, AlN);
- thin films and coatings (*e.g.* silicides);
- functionally graded materials (FGM) (*e.g.*TiC+Ni);
- composite materials, cermets (*e.g.* TiC+Al_2O_3, Ni+YSZ);
- complex oxides with specific magnetic or electrical properties (*e.g.* $BaTiO_3$, $YBa_2Cu_3O_{7-x}$).

The general requirement for the application of this technique is the presence of a highly exothermic synthesis reaction, although a detailed analysis of all factors involved in the formation and propagation of stable reaction fronts is quite complex. In the following section we will briefly discuss these considerations. A recent modification of the technique allows to overcome, in part, the need of a large exothermic reaction through the application of an external applied field. This new approach will be reviewed in some details in the second part of this paper.

Controlling reaction parameters

Adiabatic temperature

Figure 1 depicts the typical macroscopic steps of a CS process. The pellet of the reactants is generally ignited from the top and the combustion front propagates towards the bottom leaving behind the reaction products. In an idealized representation the trend of macroscopic parameters representing the combustion process are reported in Figure 2(a). The reaction is limited to a very narrow region, 10-50 μm wide, in which the degree of conversion (η) goes rapidly from 0 to 1 while the temperature increases to its maximum theoretical value, the adiabatic combustion temperature (T_{ad}). Heat is conducted ahead of the combustion front and the temperature corresponding to the onset of the chemical reaction is generally referred to as the ignition temperature (T_{ig}). The symbol ϕ in Figure 2(a) represents the rate of heat release, corresponding to the rate of the chemical process. In real processes, however, the reaction zone can be wider. This happens in the case of processes with a kinetic limitation. In this case the chemical reaction continues after the passage of the combustion front producing the so-called after-burn phenomenon (Figure 2b).

Generally the presence of a largely exothermic reaction is considered an essential prerequisite for the feasibility of a combustion synthesis process. It is largely accepted that as an empirical rule of thumb self-sustaining processes cannot take place unless T_{ad}>1800K. However, there are noteworthy exceptions. Several highly exothermic processes (with high T_{ad}) cannot produce self-sustaining combustion (*e.g.* the synthesis of TaC, Nb_5Si_3, and Al_2O_3 from the elements). Over the past two decades, investigations have demonstrated that CS reactions are complex processes, even more complex than gas-phase combustion, and their occurrence depends largely on the microscopic details of the reaction mechanism. Despite that, the adiabatic combustion temperature (T_{ad}) is still widely used in defining the feasibility of a CS process. It can be easily calculated for a given chemical process on the basis of its thermodynamic characteristics and the thermophysical properties of the products. The T_{ad} is the maxi-

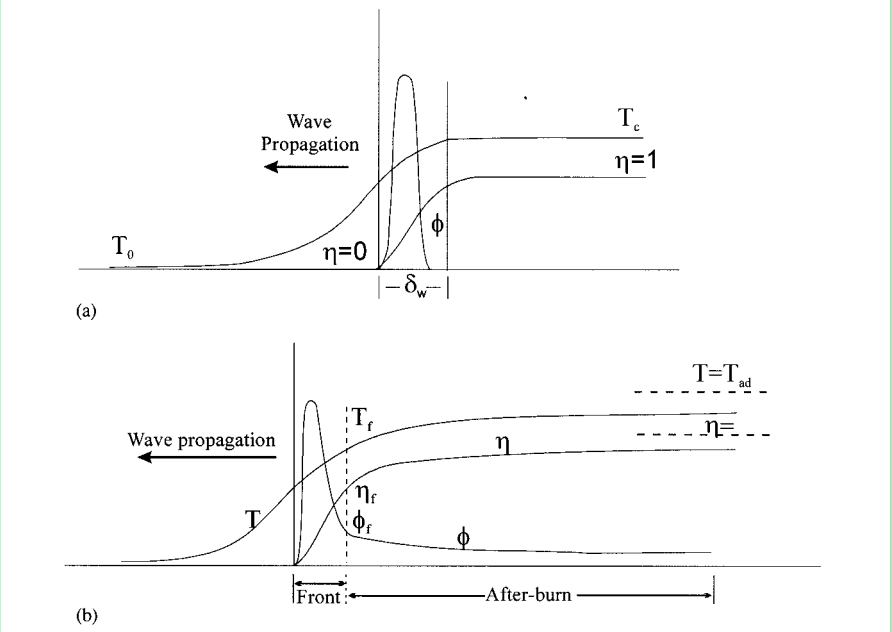

Figure 2 - Schematic representation of the temperature T, degree of conversion η, and rate of heat generation Φ, in an idealized combustion wave (a) and in presence of an after-burn (b) [3]

mum temperature to which the product can be raised if the exothermic reaction is performed in adiabatic conditions. Its value can be calculated on the basis of the following general Equation [5]:

$$\Delta H_{f,298} = \int_{298}^{T_{ad}} C_p dT \quad (1)$$

where $\Delta H_{f,298}$ is the enthalpy of the reaction and C_p is the sum of the heat capacity of the reaction products. Equation (1) is valid only when the products are all solids and do not undergo phase transitions. In the case of phase transitions and partial or total melting of products Equation (1) is modified as follows:

$$\Delta H_{f,298} = \int_{298}^{T_t} C_p(\alpha)dT + \Delta H_t + \int_{T_t}^{T_m} C_p(\beta)dT + \nu\,\Delta H_m + \int_{T_m}^{T_{ad}} C_p(liq)dT \quad (2)$$

where α and β are two different phases of the solid product, T_m is the melting point of the β phase, ΔH_t is the heat of transition between the α and the β phase, ΔH_m is the heat of fusion of the β phase, ν the fraction of solid β that is melted, and $C_p(liq)$ is the heat capacity of the liquid product.
The temperature of the combustion front is generally lower than the adiabatic temperature due to heat loss. This is shown in Table 2, where the values of adiabatic temperature and of the measured combustion temperature are compared for a number of selected reactions. Since heat loss depends on the surface area/volume ratio of the reacting samples, the difference between adiabatic and experimental combustion temperatures decreases with an increase in sample size (Figure 3).

Table 2 - [9]

Reaction	T_{ad}*(K)*	T_{exp}*(K)*
Ni+Al→NiAl	1910	1910
Co+Al→CoAl	1900	1880
Ti+Si→TiSi	2000	1850
Ti+2Si→$TiSi_2$	1800	1770
Nb+2Si→$NbSi_2$	1900	1880
5Ti+3Si→Ti_5Si_3	2500	2350
Nb+C→NbC	2800	2650
2Ta+C→Ta_2C	2600	2550

Ignition conditions
In contrast with the adiabatic temperature the ignition temperature cannot be easily calculated. It represents a very complex quantity strictly related not only to the thermodynamics and the thermophysics of the system, but also to the details of the reaction mechanism. As a general rule, ignition of a CS process is obtained when a small but significant layer of reactant powder is heated rapidly above the temperature where the rate of the chemical reaction is high enough to obtain a heat release higher than dissipation. Depending on the combination of the system parameters and of the heating rate, three different regimes can be obtained:

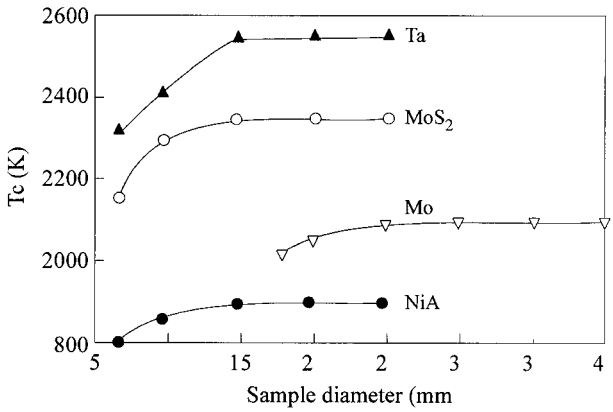

Figure 3 - Combustion temperature as a function of pellet diameter for various mixtures [3]

1) if the heating rate is too slow in comparison with the reaction rate, the reaction products are formed at a low rate through solid-solid interaction and the evolved heat is dissipated to the surrounding. This regime is very similar to the usual solid-state synthesis;
2) if the heating rate is too high only a very thin layer on the surface is heated and no self propagating process is observed, due to the limited overall release of heat. This situation is frequently observed when power laser pulse is used for the ignition. In this case localized fusion and even vaporization of the reactants is observed without ignition;
3) if the heating rate is high in comparison with the rate of the chemical process, but is slow in comparison with the heat conductivity of the sample, the heating will not be localized near the surface but the entire sample will be heated. In this situation the chemical process will start at the same time throughout the entire pellet. This regime is generally indicated as volume combustion or thermal explosion. In this case no propagating front is observed.

None of these regimes represents the ideal ignition condition.
It must be noted that the ignition temperature varies considerably for the same reaction depending on the ignition procedure. As noted by Trambukis and Munir [10] if the heating rate is slow considerable solid-solid interactions between the reagents can take place during heating, reducing the possibility of ignition of the combustion process due to the presence of the passivating layer at the interface between the powder particles.
Despite its importance in defining the reaction conditions, ignition has received relatively little attention from both theoretical and experimental points of view. Determination of the ignition temperature shows experimental challenges and has been only successfully accomplished in a very limited number of reactions. The ignition procedures used in practical CS processes do not generally allow any control of the energy supplied or the surface temperature; ignition conditions are determined in a totally empirical way. Generally, ignition is obtained using radiant energy from an electrically heated wire of a refractory metal such as W or Ta, but several other methods have been proposed, such as power lasers, electric discharge, and accessory chemical processes [5, 8].

Degree of dilution

The value of T_{ad} of a process can be modified to some extent. If the temperature of the reactants is raised above room temperature before ignition the combustion temperature will be also increased [Equations (1) and (2)]. In other words, sample preheating can be used to increase the combustion temperature. This practice is fairly common in the case of low exothermic reactions, when is difficult to obtain self-propagating reactions. On the other side, the combustion temperature can be reduced through the addition of inert phases to the reacting mixture. This procedure reduces the overall release of heat per unit volume of the mixture and takes up some of the generated heat. Dilution is a very common practice in cases of extremely exothermic processes (*e.g.* thermite reactions), when the combustion temperature is so high that it exceeds the boiling temperature of the product, resulting in explosive behavior. The products of the same reaction are generally used as diluents, in order to avoid polyphasic products. Figure 4 shows the influence of dilution on the reaction temperature in the case of the CS of TiC.

Green density

The degree of compaction of the reaction pellets strongly influences the reaction characteristics and the product microstructure. An increase in green density produces better contact between the grains of the reacting powders, but also increases the thermal conductivity. The two phenomena produce opposite effects on CS processes. The increase in grain contact enhances the overall reaction rate and the degree of its completion, but a higher thermal conductivity increases heat conduction away from the reaction front reducing the possibility for the process to remain self-sustaining. This last effect is particularly relevant for metallic reactants, where very high values of thermal conductivity are obtained for dense samples. It is well known in the case of the synthesis of intermetallic compounds that self-propagating processes are not possible for low values of the green porosity. As a result of the presence of these two competing factors in several cases an optimum value of green density is observed. Corresponding to this optimum density, a maximum in the reaction propagation rate

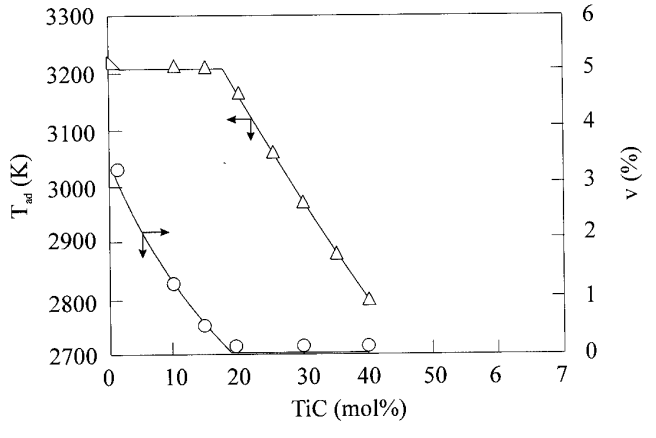

Figure 4 - The influence of addition of TiC as a diluent on the adiabatic temperature and the fraction of the melted product [4]

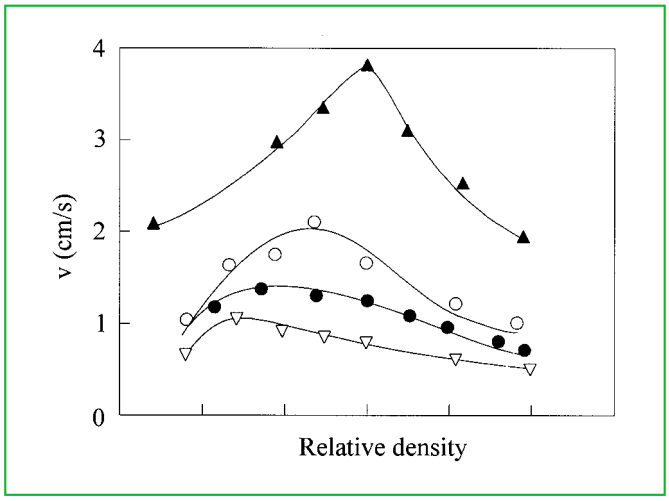

Figure 5 - The dependence of the combustion rate on the relative density of Ti+3B mixtures with different titanium particle size. From top to bottom: 300 mm, 820 mm, 1.150 mm, 1.650 mm [3]

is generally observed (Figure 5).

The sample porosity plays an obvious crucial role in the case of solid-gas combustion processes, as in the case of the synthesis of nitrides and oxides. In this case only the external surface of the sample has direct access to the gas while the conversion of the sample core requires permeation of the gaseous reactant through the pores. In this case a surface combustion is generally observed followed by a long after-burn. As a result, a very high degree of porosity is required in order to attain full conversion of the solid reactant. However, when the T_{ad} of the reaction is higher than the melting point of the reacting metal, the use of a highly porous sample results generally in a poorly converted sample. This behavior can be explained on the basis of the higher extent of melting of the reacting metal due to the higher degree of heat release in low density samples. The melting of the metal causes a reduction in the porosity resulting in a largely unconverted sample core. This behavior is well represented in the case of the synthesis of TiN were a maximum is observed in the dependence of the degree of conversion of the sample on relative density (Figure 6).

Changes in the sample green density affect also to some extent the microstructure of the final products. Examples have been found in the synthesis of some intermetallic phases, particularly aluminides, where the spreading of the low-melting reactant through the pores plays a major role in defining the characteristics of the final products.

Particle size

Along with sample porosity particle size plays a major role in defining the characteristics of the reacting mixtures and of the reaction conditions. Since the stability of the combustion front depends largely on the rapid kinetics of heat generation, it must be expected that CS processes are generally favored in smaller particle size reactants. However, the details of the dependence of the reaction characteristics on the reactants particle size are quite complex and have been studied in depth only for a few processes, such as the synthesis of TiC and of a few intermetallic compounds. Generally, it is confirmed that an increase in particle size results in a marked decrease in the propaga-

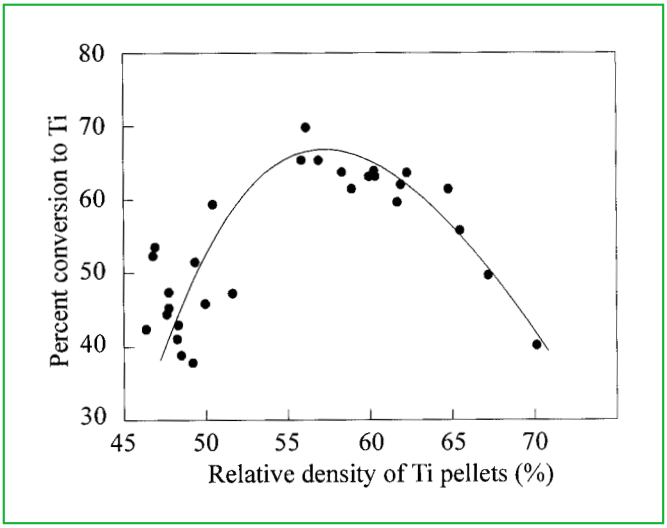

Figure 6 - The effect of relative density of Ti compacts on the degree of conversion of TiN [3]

tion rate of the reaction front (Figure 7). However, it should be kept in mind that in most combustion synthesis processes one or more of the reactants, generally the metals, melt. In such a case no dependence on the particle size of that reactant is generally observed. A typical example is represented by the synthesis of aluminides. Melting of the metal is expected also in the case of the synthesis of TiC. Despite that, a quite strong dependence of the combustion rate on Ti particle size is observed. In this case, however, it has been proposed that two different mechanisms controlling the advancement of the reaction front (diffusional or capillary spreading) are active depending on the particle size of the reactants.

But the particle size of one of the reactants can control other aspects of the combustion process. It has been reported, for example, that the particle size can influence the reaction completion, the mode of combustion (stable/unstable), and the composition of the product. In the case of the synthesis of Ti_5Si_3 the desired phase was obtained only for values of the Ti particle size <100 μm; larger particle size resulted in a product which is a mixture of Ti and $TiSi_2$ phases [5].

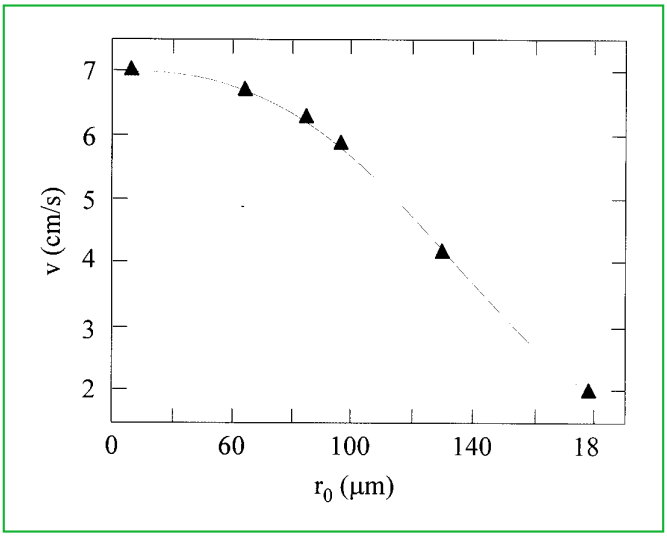

Figure 7 - Effect of particle size on the rate of combustion in the Ti+2B system [3]

Experimental setup

The experimental apparatus used in CS experiments is usually very simple. It is represented by an environmental chamber, allowing the control of the atmosphere, and by an ignition device, usually an electrically heated tungsten coil. Several other setups have been proposed with the main objective to obtain densification and shape formation of the final product. Products of CS processes are generally well sintered but highly porous (>50%). The final porosity is the sum of contributions including the original porosity of the green pellet and other sources active during the process itself [11]. These include the contribution from the decrease in molar volume, from gas evolution due to the expulsion of volatile impurities, and from the thermal migration resulting from the extremely steep thermal gradients. For some applications, such porous products can be highly desirable. These include their use as filters for corrosive or high-temperature liquids or in applications requiring high specific surface area (*e.g.* in cell applications). In most cases, however, the desire is to obtain dense, near net-shaped product. Three approaches have been used in order to increase the relative density of the products [2]:

a) simultaneous synthesis and sintering (pressurless sintering);
b) the application of pressure during or shortly after the passage of the combustion front;
c) the use of liquid phases in order to promote the formation of cast (dense) bodies.

Of these three approaches only the one relying on the application of pressure during or shortly after the combustion process has been demonstrated to be efficient and general enough to be applied to the synthesis of near net-shaped and fully dense specimen of a large class of hard materials. The heat produced by the CS processes can be large enough to bring the entire reacted sample to a temperature well above its ductile-brittle transition point and even its melting point. In such a condition even a reduced load applied to the sample can produce a very efficient densification. Figure 8 shows the schematic of a very simple apparatus that has been successfully utilized in the production of nearly fully dense TiC and TiB_2. In addition to uniaxial pressing, other methods of load application have been used. These include high speed forging and shock consolidation. Cameron *et al.* [12] have shown that using

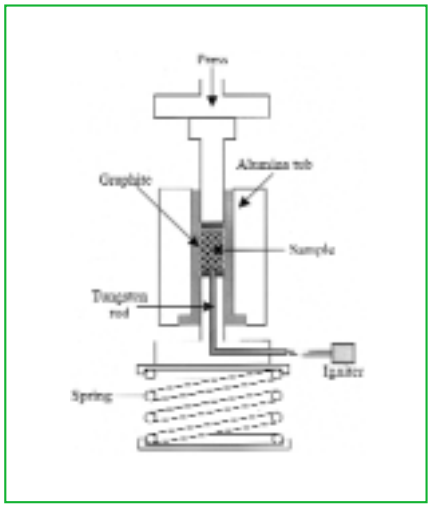

Figure 8 - Schematic of a simple apparatus used for the production of dense materials through CS

uniaxial pressing coupled with CS was possible to obtain hard composite materials (Al_2O_3-TiC, Al_2O_3-TiB_2, and Al_2O_3-B_4C/SiC) with mechanical properties and relative densities very close to those obtained on conventionally hot-pressed samples, but with a significant reduction in the complexity of the experimental apparatus. Particularly interesting for the synthesis of nearly net-shaped samples is the coupling between combustion synthesis and hot-isostatic pressing (HIPing). This method, originally proposed by Holt *et al.*[13] has been since investigated by several Japanese researchers.

Theoretical considerations

A relatively simple theory for the propagation of solid combustion wave can be derived from the classical theory of Fourier [1]. In this approach the propagation of the combustion front is described on the basis of the following heat balance and kinetic equations:

$$\rho C_p \frac{fT}{ft} = \chi \frac{f^2T}{fx^2} + Q\rho\Phi(T,\eta) - \frac{2\alpha}{R_c}(T - T_0) - \frac{2\sigma\varepsilon}{R_c}(T^4 - T_0^4) \quad (3)$$

$$\Phi(T,\eta) = \frac{f\eta}{ft}$$

where T and η represent, respectively, the temperature and the degree of conversion of the reaction, C_p is the product specific heat, ρ is the density, χ is the thermal conductivity, t is time, x is the coordinate along which the wave is propagating, Q is the enthalpy of the reaction, α the heat transfer coefficient, R_c the radius of the cylindrical pellet, ε the specific emissivity, and σ the Stefan-Boltzmann constant. The function Φ represents the rate of heat generation, corresponding to the rate of the chemical reaction. The Fourier relationship includes a term representing the rate of heat accumulation in the wave (left-hand side) and terms (right-hand side) representing the rate of the net thermally conducted heat, the rate of heat generated by the chemical process, and the rates of conductive and radiative heat losses. An analytical solution for such equations have been obtained under the assumption of negligible heat losses (adiabatic conditions), a narrow width of the wave in comparison with the thermally affected zone, and of a rate of heat release represented by the following expression:

$$\frac{\partial\eta}{\partial t} = K_0 \exp\left(-\frac{E_{att}}{RT}\right)(1-\eta)^n \quad (4)$$

where E_{att} is the apparent activation energy of the process and *n* is the order of the reaction. Under these assumptions the analytical solution of Equation (3) is:

$$u^2 = f(n)K_0 \frac{C_p\chi}{Q}\frac{RT_c^2}{E_{att}}\exp\left(-\frac{E_{att}}{RT_c}\right) \quad (5)$$

where *f(n)* represents a function depending on the reaction order. This solution shows the strong dependence of the propagation rate on the apparent activation energy, generally considered related to the activation energy of the rate-determining step in the overall process. This relationship has been also used for the experimental determination of the apparent activation energy of the combustion processes. If the combustion temperature can be changed without altering the reaction mechanism (*e.g.* through the addition of diluents) and the corresponding changes in propagation rate are determined, the apparent activation energy can be easily calculated, on the basis of Equation 5, through a plot of $\ln(u/T_c)$ *vs.* $1/T_c$.

However, due to its simplified assumptions, this treatment presents several major limitations and is generally insufficient in describing all the characteristics of a typical CS process. The kinetic function, Equation (4), for instance, is the same used in the theory of gas-phase combustion. It considers the process as a homogeneous chemical reaction, without taking into account the real microscopic reaction mechanism of CS processes that generally involves a polyphasic mixture of condensed phases with a complex microstucture. Furthermore, with this simplified approach it is not possible to take into account the large variety of propagation modes observed when CS reactions get close to extinction [3]. In fact, aside from the steady-state propagation mode, characterized by a movement of the combustion front with a constant velocity throughout the sample, other more complex propagation modes are frequently observed. The most common is represented by the pulsating mode. In this mode, observed also in gas-phase combustion, the movement of the combustion front is characterized by the succession of rapid and slow displacements, with this oscillation being either periodic or chaotic. Another typical instability is represented by the spin mode. Here the reaction is limited to a small region that propagates in a spiral motion around the sample. Spin combustion is a peculiarity of the CS process and does not have a correspondence in gas-phase combustion. A great deal of theoretical work has been dedicated to the analysis of these irregularities. This effort, however, was mainly directed towards the analysis and representation of the macroscopic phenomenology, while only little attention was paid to the microscopic aspects of the reaction mechanism. An effort in this direction has been made for the synthesis of some carbides [14] and oxides [15]. In these cases the macrokinetic Equation (3) has been coupled with a microkinetic function based on a realistic model describing the reactivity of the single grains of the reactants.

Effect of an Electric Field on Self-Propagating Reactions

Experimental and Modeling Studies

The need to activate SHS reactions by an electric field is necessitated by the intrinsic characteristics of some of these processes. The limitations of SHS reactions can be classified as thermodynamic or kinetic. A low value of heat of reaction represents a thermodynamic limitation. Kinetic limitations are manifested by a non-optimum value of heat conductivity or a low reaction rate. In principle, as we said previously, the limitations of SHS reactions can be overcome by thermal activation, *i.e.*, by raising the temperature of the reactants to achieve a higher adiabatic temperature. But in practice such an approach is often undesirable because of the formation of pre-combustion reaction phases

before the onset of the main reaction, a circumstance that modifies the process [16, 17].
A more direct method of activation involves the application of an electric field. As will be shown later, in many systems this form of activation delivers an additional (electric) energy directly to the reaction zone. In the presence of the externally applied field, the Fourier Equation (1) is modified as follows:

$$\rho C_p \frac{\partial T}{\partial t} = \kappa \frac{\partial^2 T}{\partial x^2} + q_c + q_e \qquad (6)$$

where q_c ($=\rho Q \partial\eta/\partial t$) is the rate of chemical heat release and q_e is the rate of electrical heat release with $q_e=\sigma E^2$, where σ is the electrical conductivity and E is the electric field. A schematic representation of field activation is shown in Figure 9. The reactant mixture is placed between two electrodes and a voltage is applied across them. Simultaneously, an ignition source is activated near one end of the sample.
Field activation of SHS has been shown to have a dramatic effect on the dynamics of the process and on the nature and composition of the product(s) [18]. From a phenomenological point of view, the application of a field has many advantages, among which are the following:
- makes possible the synthesis of monolithic and composite materials which could not heretofore be prepared by SHS [19, 20];
- extends the compositional limits of composites that can be formed by SHS [21,22];
- influences the composition of the product phase(s) [23-25];
- influences the elemental distribution in solid solutions [23];
- makes SHS reactions possible in dense reactant media [26];
- influences the microstructure of the product of SHS [27].

At a fundamental level, the application of a field has been shown to initiate SHS combustion waves when the magnitude of the field is above a minimum (threshold) value, E_t. The value of E_t is material-specific. Once a wave is initiated, its temperature and velocity are directly dependent on the magnitude of the field, as can be seen in Figure 10 [19]. From experimental and modeling studies, it was shown that

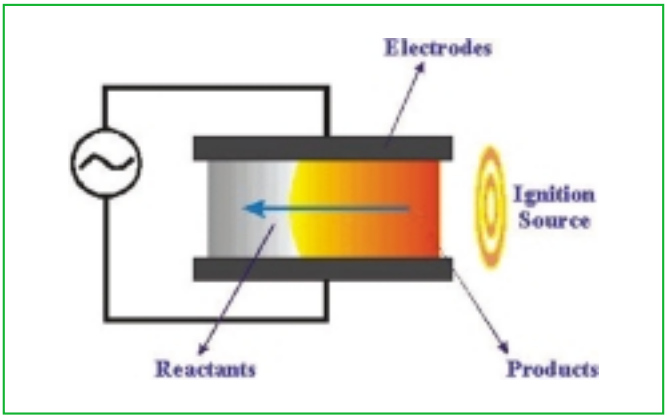

Figure 9 - Schematic of the experimental setup used for the field-assisted combustion synthesis

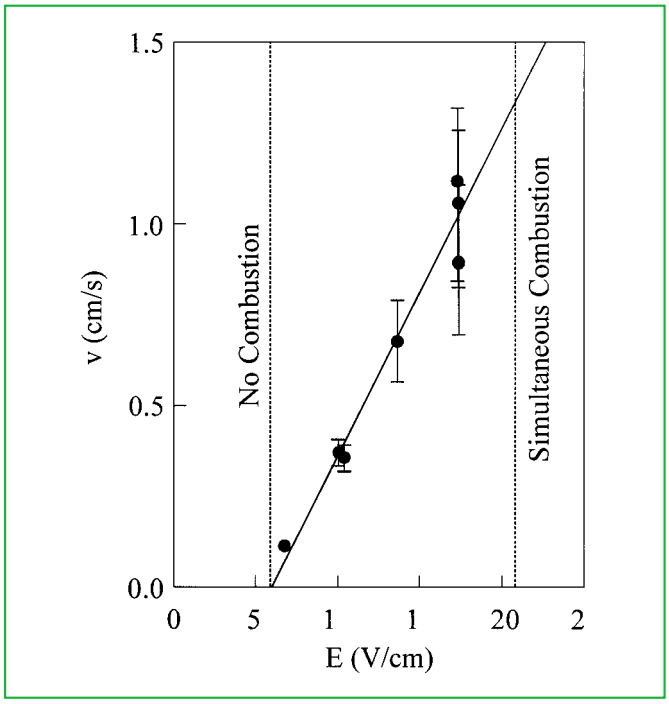

Figure 10 - Effect of the field on the velocity of the combustion wave in the synthesis of SiC [19]

the degree of activation, *i.e.* the portion of the electrical energy rate (σE^2) imparted to the wave, is governed by the electrical conductivity of the product. In systems with relatively non-conducting products, *e.g.*, SiC, the activation is nearly 100%. In such cases, the current passing through the sample is localized to the combustion zone. Indirect evidence for this is provided in Figure 11 by the constancy of the real-time voltage (and current) during wave propagation (the segment between the start, S, and end, E, of the wave). In this case the wave velocity is constant with distance of propagation. In contrast, in systems with relatively conducting products, *e.g.*, Nb_5Si_3, the degree of activation decreases with distance and the velocity shows a similar trend [28].
Modeling of field-activation was made on the basis of a

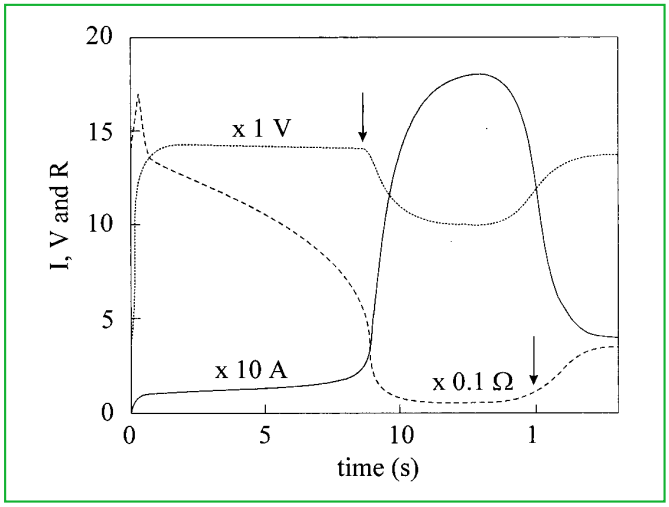

Figure 11 - Variation of the current, voltage, and resistance during wave propagation in the synthesis of SiC [28]

modified Equation (4) taking into account heat loss terms. The analysis was made in two-dimension and the parameters of heat capacity, thermal conductivity, and electrical conductivity were taken as functions of temperature and composition. Details of the modeling analysis are given elsewhere [29]. The results of the modeling studies are in qualitative agreement with the experimental observations [30]. The localization of the current to the combustion zone was clearly demonstrated for the case of SiC, in agreement with experimental observations.

The Effect of Electrical and Thermal Conductivites and Porosity on Field Activation

As indicated above, the conductivity of the product plays a major role in the extent of current localization and hence the degree of activation. Since for any materials system the thermophysical properties are, *per force,* constant, modeling is an important tool to examine their effect. Figure 12 shows the current density profiles for SiC in which the electrical conductivity is hypothetically changed. The middle sequence is for the actual conductivity, σ_0, while the upper and lower sequences are for σ/σ_0 of 0.4 and 2.5, respectively. The results clearly show the confinement of the current to the reaction zone when the conductivity is low (lower sequence). As the conductivity increases, the current becomes less confined, as can be seen in the upper sequence of Figure 12. Modeling studies were made to assess the role of electrical and thermal conductivity, and relative density (porosity) [31]. The effect of electrical conductivity on wave velocity is shown in Figure 13. The dependence of the wave velocity, v, on F_σ ($=\sigma/\sigma_0$) shows a maximum which shifts to lower F_σ values as the strength of the field is increased. The existence of a maximum is related to the degree of activation. For low σ, the contribution to the combustion front is small, since it depends on σE^2. For high σ, the contribution to the front is also small since the current is now carried by the product phase. At an intermediate value of σ, an optimum contribution to the reaction front results in a maximum velocity, as seen in Figure 13. For the case of thermal conductivity the results are similar but the reason for this behavior is different. When the conductivity is low, the rate of heat transfer to the reactant layer just ahead of the combustion zone is low and thus the portion of the sample does not reach the ignition temperature readily. This leads to a lower wave velocity. On the other hand, when the thermal conductivity is high, heat is conducted readily ahead of the wave leading to its dissipation in regions far ahead of the wave. The consequence of this is that the layer ahead of the wave does not reach ignition readily.

Similar modeling results were obtained for the effect of relative density on wave velocity [31]. Although relative density has an implied role in the heat generated (Q) and in the electrical and thermal conductivities, its role in thermal conductivity is believed to be the key factor. Several experimental studies have reported a dependence of the wave velocity on relative density showing a maximum at an optimum density. Figure 14 shows such a dependence for the case of the synthesis of $MoSi_2$. A clear maximum in the velocity is seen at intermediate densities. When the re-

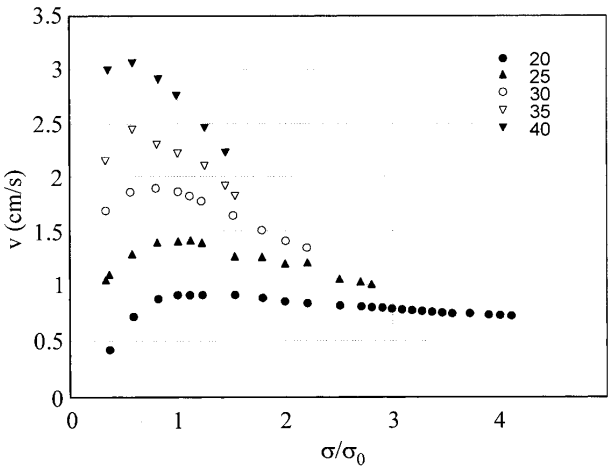

Figure 13 - Effect of electrical conductivity on combustion wave velocity [31]

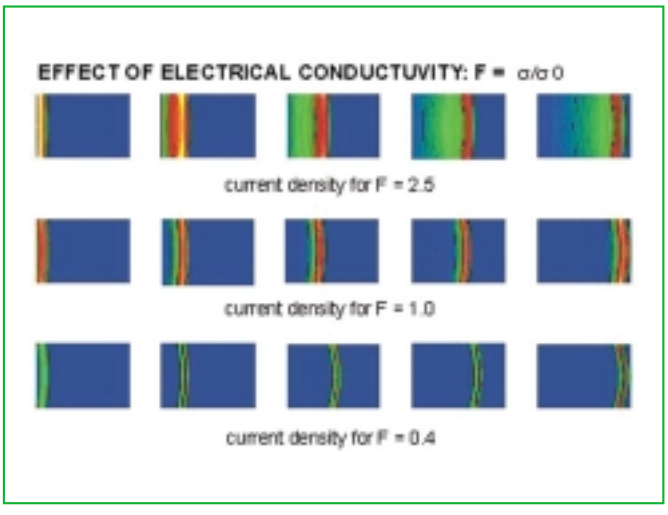

Figure 12 - Simulation of the current density distribution during the synthesis of SiC for three different values of the parameter $F=\sigma/\sigma_0$, with σ_0 indicating the real electrical conductivity of SiC [31]

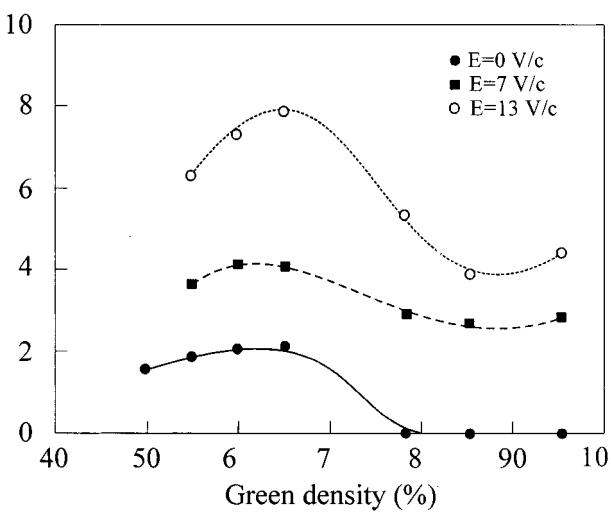

Figure14 - Influence of green density on the propagation rate for the synthesis of $MoSi_2$

actants are relatively dense (about 80% relative density), no SHS wave is possible. But as the figure shows, the application of a field changes that, making possible the propagation of SHS waves in highly dense (95%) reactants. This field effect has a practical component, by contributing to the reduction of the final porosity of SHS products through the use of dense reactants [32].

The Influence of the Field on Phase Formation during Combustion Synthesis

As was indicated above, the field plays a major role in SHS processes. In this section we focus on the influence of the field on phase formation during SHS. Three examples are briefly presented to demonstrate the role of the field:

a) the synthesis of tungsten silicides;
b) the synthesis of intermetallic phases;
c) the synthesis of composites and solid solutions.

The reactions to form the two silicides of tungsten, WSi_2 and W_5Si_3, are not sufficiently energetic to enable their synthesis by the SHS method. The adiabatic temperatures for these compounds are 1459 and 954K, respectively. But both can be synthesized by field-activated combustion synthesis, FACS, when an above-threshold field is imposed in each case [33]. When low fields (13-17 V·cm^{-1}) were applied, the synthesis of WSi_2 can be realized, but that of W_5Si_3 is not possible. Although a combustion wave is initiated, the product is a mixture of tungsten and WSi_2. However, when the reaction is carried out under higher fields (20-35 V·cm^{-1}), the desired product was synthesized. These observations provide indirect evidence of the role of the field in the mechanism of the formation reaction.

Another example of the role of the field is provided by experimental results on the synthesis of intermetallics by SHS. Generally, intermetallic compounds have low formation enthalpies and thus cannot be formed by normal SHS [34]. Furthermore, it is not always possible to initiate self-sustaining reactions in metal compacts. But in the presence of a field with an above threshold value such reactions can easily be initiated and sustained. But the most important aspect of this is the dependence of the nature of the product on the magnitude of the applied field. An example is the case of the synthesis of Ti_3Al. At a field of 5.7 V·cm^{-1} (just above the threshold), a wave propagates but the product includes many other Ti-Al phases as well as unreacted Ti [24]. As the magnitude of the field, E, is increased, the number of phases in the product decreases and when E=15.7 V·cm^{-1}, only the desired phase, Ti_3Al, is present. Similar observations have been made in the case of FeAl in which it was necessary to increase the field to 12.5 V·cm^{-1} to obtain the pure phase [25].

The last example on the effect of the field on phase formation is the synthesis of AlN-SiC composites and solid solutions. Considering more than 250 polytypes of SiC, the 2H (hexagonal) polytype forms extensive solid solutions with AlN (from about 25 to 100 mol% AlN) at temperatures above about 1960 °C. When the solutions are annealed below this temperature, a spinodal decomposition takes place resulting in a nano-modulated composite of AlN-rich and SiC-rich phases. The common method of synthesizing the solid solutions is by heating a mixture of AlN and SiC at temperatures higher than 2100 °C for up to 16 hrs. As it will be discussed briefly below, using field activation, solid solutions can be synthesized in seconds.

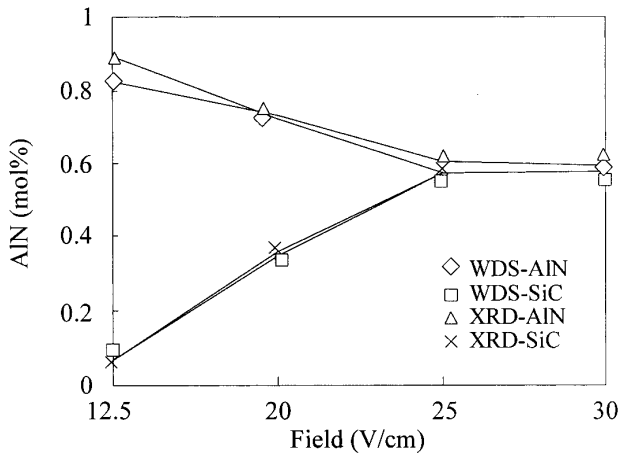

Figure 15 - Dependence of the phase compositions for the composite AlN-SiC obtained through the reaction Si_3N_4+4Al+3C→ →4AlN+3SiC as a function of the applied voltage [23]

Formation of solid solutions and composites of AlN-SiC was investigated through the reaction Si_3N_4+4Al+3C →4AlN+3SiC [23]. Although T_{ad} for this reaction is high (2504K), the reaction is not self-sustaining, but can become so in the presence of an above-threshold field of 8.0 V·cm^{-1}. However, as in the case of intermetallic synthesis discussed above, wave propagation near threshold fields resulted in incomplete reactions. As the field increased, the reaction became complete and the product contained AlN-rich and SiC-rich phases. As the field increased further, the compositions of these two phases approached each other, and when E=25.0 V·cm^{-1}, the compositions of both phases were identical, *i.e.,* a solid solution has formed. These results are shown in Figure 15. With further increase in the field to 30.0 V·cm^{-1}, the composition (as determined from X-ray diffraction) remains the same but electron microprobe analysis showed an important difference. The solid solution synthesized at E=25.0 V·cm^{-1} has considerable non-uniformity in the elemental distributions. But when E=30.0 V·cm^{-1}, the solution exhibited nearly perfect uniformity as judged by the EPMA results. These observations show another important role played by the field in the process of phase formation during SHS.

Simultaneous Synthesis and Densification by Field Activation

As indicated above, the products of SHS are generally porous, with the porosity originating from different sources, as has been discussed elsewhere [32]. Although for some applications this is a desirable outcome, for many others it is a significant disadvantage, as was pointed out previously. Until recently, products of SHS were subjected to a secondary step to achieve high densities. Recently, however, it was demonstrated that through field activation the products can be synthesized and consolidated simultaneously. This approach has been used to prepare dense materials such as $MoSi_2$, Ti_3SiC_2, TiB_2-WB_2-CrB_2 solid solutions, and others. More recently, this method has been extended to synthesize dense nanomaterials. ◆

References

[1] A.G. Merzhanov, I.P. Boroviskaya, *Dokl. Acad. Sci. USSR. (Chem.),* 1972, **204,** 429.
[2] Z.A. Munir, *Am. Ceram. Soc. Bull.,* 1988, **67,** 342.
[3] Z.A. Munir, U. Anselmi-Tamburini, *Mater.Sci. Reports,* 1989, **3,** 277.
[4] J.B. Holt, Z.A. Munir, *J. Mater. Sci.,* 1986, **21,** 251.
[5] A. Varma, J-P. Lebrat, *Chem. Eng. Sci.,* 1992, **47,** 2179.
[6] A.G. Merzhanov, *Comb. Sci. Technol.,* 1994, **98,** 307.
[7] J.J. Moore, H.J. Feng, *Progress in Materials Science,* 1995, **39,** 243.
[8] J.J. Moore, H.J. Feng, *Progress in Materials Science,* 1995, **39,** 275.
[9] J. Subrahmanyam, M. Vijayakumar, *J. Mater. Sci.*, 1992, **27,** 6249.
[10] J. Trambukis, Z.A. Munir, *J. Amer. Ceram. Soc.,* 1990, **73,** 1240.
[11] Z.A. Munir, *J. Mater. Synth. Process.,* 1993, **1,** 387.
[12] C.P. Cameron, J.H. Enloe *et al., Ceram. Engng. Sci. Proc.,* 1990, **11,** 1190
[13] J.B. Holt, *MRS Bulletin,* 1987, **15,** 60.
[14] A.M. Kanury, *Metall. Trans.,* 1992, **23A,** 2349.
[15] M. Arimondi, U. Anselmi-Tamburini, A. Gobetti, Z.A. Munir, G. Spinolo, *J. Phys. Chem.* 1997, **B101,** 5059.
[16] S.C. Deevi, *Mater. Sci. Eng.,* 1992, **149,** 741.
[17] D.C. Halverson, Z.A. Munir, B.Y. Lum, in "Combustion and Plasma Synthesis of High Temperature Materials", Z.A. Munir, J.B. Holt, (Eds.), VCH Publishers, NY (1990).
[18] Z.A. Munir, W. Lai, K.H. Ewald, *US Pat.* 5,380,409, January 10, 1995.
[19] A. Feng, Z.A. Munir, *Metall. Mater. Trans.,* 1995, **26B,** 587.
[20] H. Xue, Z.A. Munir, *Int. J. SHS,* 1996, **5,** 229.
[21] H. Xue, Z.A. Munir, *Metall. Mater. Trans.,* 1995, **27B,** 475.
[22] S. Gedevanishvili Z.A. Munir, *Mater. Sci. Eng.,* 1998, **A242,** 1.
[23] H. Xue, Z.A. Munir, *J. Europ. Ceram. Soc.,* 1997, **17,** 1787.
[24] R. Orru, G. Cao, Z.A. Munir, *Metall. Mater. Trans.,* 1999, **30A,** 1101.
[25] K. Kawase, Z.A. Munir, *Int. J. SHS,* 1998, **7,** 95.
[26] H. Xue, K. Vandersall, E. Carrillo-Heian, Z.A. Munir, *J. Amer. Ceram. Soc.,* 1999, **82,** 1441.
[27] Z.A. Munir, in "Molybdenum and Molybdenum Alloys", A. Crowson, E.S. Chen *et al.,* (Eds.), TMS, Warrendale, PA, 1998, 49.
[28] A. Feng, Z.A. Munir, *J. Amer. Ceram. Soc.,* 1997, **80,** 1222.
[29] A. Feng, O.A. Graeve, Z.A. Munir, *Comput. Mater. Sci.,* 1998, **12,** 137.
[30] A. Feng, Z.A. Munir, *Metall. Mater. Trans.* 1995, **26B,** 581.
[31] E.M. Carrillo-Heian, O.A. Graeve *et al., J. Mater. Res.,* 1999, **14,** 1949.
[32] S. Gedevanishvili, Z.A. Munir, *J. Mater. Res.,* 1995, **10,** 2642.
[33] Z.A. Munir, D. Odink, Proceedings of second International Symposium on Metallurgical Processes for the Year 2000 and Beyond, H.Y. Sohn, (Ed.), TMS, Warrendale, PA, 1994, 167.
[34] Z.A. Munir, I.J. Shon, K. Yamazaki, *US Pat.* 5,794,113, August 11, 1998.